IEEE Access
Multidisciplinary | Rapid Review | Open Access Journal

Received September 26, 2019, accepted October 13, 2019, date of publication October 21, 2019, date of current version October 31, 2019.

Digital Object Identifier 10.1109/ACCESS.2019.2948634

Parallel Lattice Structure for Dual Windows Computation in Multiwindow Gabor Transform

RUI LI[1] AND HON KEUNG KWAN[2], (Life Senior Member, IEEE)
[1]College of Information and Network Engineering, Anhui Science and Technology University, Bengbu 233030, China
[2]Department of Electrical and Computer Engineering, University of Windsor, Windsor, ON N9B 3P4, Canada

Corresponding author: Rui Li (lir@ahstu.edu.cn)

This work was supported in part by the Provincial Science and Technology Major Project of Anhui under Grant 18030901022, and in part by the Natural Science Foundation of Anhui Science and Technology University under Grant XWYJ201802.

ABSTRACT The multiwindow discrete Gabor transform (M-DGT) is a useful time-frequency analysis tool for non-stationary signal processing. Given an arbitrary Gabor frame, a parallel lattice structure of block time-recursive algorithm for fast and efficient computation of dual/analysis Gabor windows for M-DGT is presented. By using a multiple window dual Gabor frame, the dual Gabor windows can be expressed by synthesis and analysis windows with a block-circulant matrix. Then, a parallel lattice structure of block time-recursive can be derived to solve the dual Gabor windows by the block-circulant matrix computed by the fast discrete Fourier transform (FFT). When compared to three existing methods, the proposed algorithm can reduce computational complexity and save computational time. Experimental results indicate that the proposed algorithm is valid to compute the dual windows of the M-DGT, which make the algorithm attractive for fast time-frequency signal analysis and processing.

INDEX TERMS Multiwindow discrete Gabor transform (M-DGT), parallel lattice structure, block time-recursive methods, dual (analysis) Gabor windows, block-circulant matrix, time-frequency analysis.

I. INTRODUCTION

The Gabor transform (GT) [1] is a widely-utilized time-frequency analysis tool to represent, analyze, and process signal which can be constructed from a window function by translation in both time domain and frequency domain. Recently, various advances have emerged in fast computing algorithms for discrete Gabor transform [2], [3] and fast computing algorithms for real-valued discrete Gabor transform [4]–[8]. There has also been an expanding scope of applications which include for examples, audio processing [9]–[11], speech processing [12], ultrasound processing [13], noise reduction for NMR FID signals [14], image processing [15]–[17], face recognition [18], [19], object recognition [20], [21], and so on. However, due to the Heisenberg uncertainty principle, the Gabor representation with a single window is insufficient to analyze signals with dynamic time-frequency components. To solve this issue, multiwindow Gabor analysis using multiple windows with different time-frequency localizations has been utilized to process multiple frequency components of a signal.

The associate editor coordinating the review of this manuscript and approving it for publication was Yue Zhang.

Computing the Gabor dual/analysis windows involve inverting a matrix operator associated with a given Gabor frame composed by synthesis windows. Recently, A number of studies on Gabor dual windows have been presented [22]–[27]. A method for solving Gabor dual windows with linear constraints was proposed in [28]. By using the duality and support conditions of the Gabor frame [29], a linear system can be devoted to compute the Gabor dual windows based on Moore-Penrose pseudo inverse. Also an optimal modified ℓ_2 norm for finding Gabor dual windows was presented in [30]. To solve the Gabor dual windows problem of the M-DGT, a method based on multi-Gabor frame was presented in [31]. On the other hand, a number of bi-orthogonal analysis methods with ℓ_2 norm constraints [32]–[35] derived from the completeness condition of the M-DGT, have been presented to compute the analysis windows of the M-DGT. Nevertheless, all the above methods involve an inverse matrix calculation problem. If such a matrix has large dimensions, it could lead to computational instability and requires a huge amount of memory and computation. To over this issue, the FFT was used in [36] to compute the dual window in the DGT, which can avoid computing the inverse matrix of a given frame. The parallel lattice

structure of a block time-recursive method was presented in [37] to compute the dual/analysis window of the DGT for a constructed Gabor frame, but can only apply to a window function that can form a Gabor frame. The above methods only address the dual/analysis window problem of the DGT in a serial computing mode or are limited to constructing a Gabor frame. However, a fast parallel computation of the dual/analysis of the M-DGT has not been addressed.

In this paper, an efficient algorithm for computing the Gabor dual windows of the M-DGT is proposed for a given multiwindow Gabor frame, in which the inversion of a Gabor frame matrix with block circulant characters can be computed by the FFT, followed by the design of the parallel lattice structure of the block time-recursive method for implementation. The proposed algorithm does not require a matrix inversion which is computationally intensive especially when the associated matrix dimensions are high. The proposed algorithm is simple to be implemented in software or hardware. Analysis of the computational complexities of the proposed algorithm and other algorithms clearly show that the proposed algorithm can provide a faster approach to compute the Gabor dual windows in the M-DGT.

The rest of the paper is organized as follows. In section II, the equations required for computing the multiwindow Gabor system will be given. In section III, the block time-recursive method for computing the Gabor dual windows of the M-DGT will be used to design the unified parallel lattice structure for implementing the proposed algorithm. In section IV, a detailed analysis and comparison will be given to demonstrate the amount of computational savings of the proposed algorithm as compared to other existing algorithms. Section V will present computational examples and results. Finally, conclusions are given in section VI.

II. MULTIWINDOW GABOR FRAME

Let $\boldsymbol{f}$ be periodic sequences of length L, the standard dual frame of the multiwindow Gabor representation [31], [36], [38], [39] is defined as (1).

$$\mathcal{S}\boldsymbol{f} = \sum_{p=0}^{P-1}\sum_{m=0}^{M-1}\sum_{n=0}^{N-1}\left\langle \boldsymbol{f}, \boldsymbol{g}_{m,n}^{(p)}\right\rangle \boldsymbol{g}_{m,n}^{(p)}, \tag{1}$$

where $\mathcal{S}$ be the frame operator for synthesis sequences $\left\{\boldsymbol{g}_{m,n}^{(p)}\right\}$ formed by translations and modulations of windows $\boldsymbol{g}$ as in (2).

$$g_{m,n}^{(p)}(k) = g^{(p)}\left(k - m\bar{N}\right)\exp\left(\frac{j2\pi nk}{N}\right)$$
$$0 \le m \le M-1,\ 0 \le n \le N-1,\ 0 \le p \le P-1, \tag{2}$$

where $j = \sqrt{-1}$, $\bar{N}$ is the time translation step, N is the number of frequency sampling bins, and $L = M\bar{N} = \bar{M}N$. If the frame operator $\mathcal{S}$ is invertible, then (1) can be rewritten as (3).

$$\boldsymbol{f} = \sum_{p=0}^{P-1}\sum_{m=0}^{M-1}\sum_{n=0}^{N-1}\left\langle \boldsymbol{f}, \mathcal{S}^{-1}\boldsymbol{g}_{m,n}^{(p)}\right\rangle \boldsymbol{g}_{m,n}^{(p)}, \tag{3}$$

and let

$$\gamma_{m,n}^{(p)}(k) = \mathcal{S}^{-1}g_{m,n}^{(p)}(k) = g^{(p)}\left(k - m\bar{N}\right)\exp\left(\frac{j2\pi nk}{N}\right)$$
$$0 \le m \le M-1,\ 0 \le n \le N-1,\ 0 \le p \le P-1, \tag{4}$$

be the dual multiwindow analysis sequences of a multiwindow Gabor system, where

$$\boldsymbol{\gamma}^{(p)} = \mathcal{S}^{-1}\boldsymbol{g}^{(p)}. \tag{5}$$

The multiwindow discrete Gabor expansion (M-DGE) can be defined as (6).

$$f(k) = \sum_{p=0}^{P-1}\sum_{m=0}^{M-1}\sum_{n=0}^{N-1} c^{(p)}(m,n)g_{m,n}^{(p)}(k), \tag{6}$$

and the transform coefficients $c^{(p)}(m,n)$ can be obtained by the multiwindow discrete Gabor transform (M-DGT) as in (7).

$$c^{(p)}(m,n) = \sum_{k=0}^{L-1} f(k)\gamma_{m,n}^{(p)}(k). \tag{7}$$

III. PARALLEL ALGORITHM FOR COMPUTING DUAL GABOR WINDOWS IN M-DGT

To derive a relationship between a window and its dual window, substituting (5) into (1) leads to

$$\begin{aligned}\boldsymbol{g}^{(p)} &= \sum_{\bar{p}=0}^{P-1}\sum_{m=0}^{M-1}\sum_{n=0}^{N-1}\left\langle \boldsymbol{\gamma}^{(p)}, \boldsymbol{g}_{m,n}^{(\bar{p})}\right\rangle \boldsymbol{g}_{m,n}^{(\bar{p})} \\ &= \boldsymbol{G}\boldsymbol{\gamma}^{(p)},\end{aligned} \tag{8}$$

where $\boldsymbol{G}$ is a $L \times L$ matrix constructed by

$$\boldsymbol{G}(k,k') = \sum_{\bar{p}=0}^{P-1}\boldsymbol{G}^{(\bar{p})}(k,k'), \tag{9}$$

where

$$\begin{aligned}&\boldsymbol{G}^{(\bar{p})}(k,k') \\ &= \begin{cases} N\sum_{m=0}^{M-1} g^{(\bar{p})}\left(k - m\bar{N}\right)g^{(\bar{p})}\left(k' - m\bar{N}\right), & N \mid |k-k'| \\ 0, & otherwise \end{cases} \\ &= \begin{cases} N\sum_{m=0}^{M-1} g^{(\bar{p})}\left(k + m\bar{N}\right)g^{(\bar{p})}\left(k' + m\bar{N}\right), & N \mid |k-k'| \\ 0, & otherwise, \end{cases}\end{aligned} \tag{10}$$

and $0 \le k \le L-1, 0 \le k' \le L-1$.

Theorem 1: Let $\boldsymbol{G}_{u,v}^{(\bar{p})}$ denote $\bar{N} \times \bar{N}$ matrix with element

$$\left(\boldsymbol{G}_{u,v}^{(\bar{p})}\right)_{r,s} = \boldsymbol{G}^{(\bar{p})}\left(r + u\bar{N}, s + v\bar{N}\right), \tag{11}$$

where $0 \le \bar{p} \le P-1, 0 \le u, v \le M-1$, and $0 \le r, s \le \bar{N}-1$. Then $\boldsymbol{G}$ can be expressed as a block right circulant matrix.

Proof: The matrix $\boldsymbol{G}^{(\bar{p})}$ can be rewritten as (12).

$$\boldsymbol{G}^{(\bar{p})}=\begin{bmatrix} \boldsymbol{G}^{(\bar{p})}_{0,0} & \boldsymbol{G}^{(\bar{p})}_{0,1} & \cdots & \boldsymbol{G}^{(\bar{p})}_{0,M-1} \\ \boldsymbol{G}^{(\bar{p})}_{1,0} & \boldsymbol{G}^{(\bar{p})}_{1,1} & \cdots & \boldsymbol{G}^{(\bar{p})}_{1,M-1} \\ \vdots & \vdots & \ddots & \vdots \\ \boldsymbol{G}^{(\bar{p})}_{M-1,0} & \boldsymbol{G}^{(\bar{p})}_{M-1,1} & \cdots & \boldsymbol{G}^{(\bar{p})}_{M-1,M-1} \end{bmatrix}. \tag{12}$$

Due to the periodicity of $g^{(\bar{p})}$,

$$\begin{aligned}\left(\boldsymbol{G}^{(\bar{p})}_{u+k,v+k}\right)_{r,s} &= \boldsymbol{G}^{(\bar{p})}\left(r+u\bar{N}+k\bar{N}, s+v\bar{N}+k\bar{N}\right) \\ &= N\sum_{m=0}^{M-1} g^{(\bar{p})}\left(r+u\bar{N}+(k+m)\bar{N}\right) \\ &\quad\times g^{(\bar{p})}\left(s+v\bar{N}+(k+m)\bar{N}\right) \\ &= N\sum_{m'=0}^{M-1} g^{(\bar{p})}\left(r+u\bar{N}+m'\bar{N}\right) \\ &\quad\times g^{(\bar{p})}\left(s+v\bar{N}+m'\bar{N}\right) \\ &= \left(\boldsymbol{G}^{(\bar{p})}_{u,v}\right)_{r,s}, \end{aligned} \tag{13}$$

and $0 \le k \le M-1$, substituting (13) into (12) leads to $\boldsymbol{G}^{(\bar{p})}$ which can be rewritten as a block right circulant matrix as

$$\begin{aligned}\boldsymbol{G}^{(\bar{p})} &= \begin{bmatrix} \boldsymbol{G}^{(\bar{p})}_{0} & \boldsymbol{G}^{(\bar{p})}_{1} & \cdots & \boldsymbol{G}^{(\bar{p})}_{M-1} \\ \boldsymbol{G}^{(\bar{p})}_{M-1} & \boldsymbol{G}^{(\bar{p})}_{0} & \cdots & \boldsymbol{G}^{(\bar{p})}_{M-2} \\ \vdots & \vdots & \ddots & \vdots \\ \boldsymbol{G}^{(\bar{p})}_{1} & \boldsymbol{G}^{(\bar{p})}_{2} & \cdots & \boldsymbol{G}^{(\bar{p})}_{0} \end{bmatrix} \\ &= \mathcal{C}\left(\boldsymbol{G}^{(\bar{p})}_{0}, \boldsymbol{G}^{(\bar{p})}_{1}, \cdots, \boldsymbol{G}^{(\bar{p})}_{M-1}\right), \end{aligned} \tag{14}$$

where

$$\boldsymbol{G}^{(\bar{p})}_{m} = \boldsymbol{G}^{(\bar{p})}\left(\cdot, \cdot + m\bar{N}\right), \tag{15}$$

and $0 \le m \le M-1$, then

$$\boldsymbol{G} = \sum_{\bar{p}=0}^{P-1} \mathcal{C}\left(\boldsymbol{G}^{(\bar{p})}_{0}, \boldsymbol{G}^{(\bar{p})}_{1}, \cdots, \boldsymbol{G}^{(\bar{p})}_{M-1}\right). \tag{16}$$

The above leads to $\boldsymbol{G}$ in the form of a block right circulant matrix thus completing the proof of Theorem 1.

In this section, an efficient algorithm will be developed to compute the dual Gabor windows without computing the inverse matrix of $\boldsymbol{G}$. According to the Theorem 1, it can be see that the matrix $\boldsymbol{G}$ has a block right circulant structure, hence $\boldsymbol{G}$ can be rewritten as

$$\begin{aligned}\boldsymbol{G} &= \mathcal{C}\left(\boldsymbol{G}_0, \boldsymbol{G}_1, \cdots, \boldsymbol{G}_{M-1}\right) \\ &= \begin{bmatrix} \boldsymbol{G}_0 & \boldsymbol{G}_1 & \cdots & \boldsymbol{G}_{M-1} \\ \boldsymbol{G}_{M-1} & \boldsymbol{G}_0 & \cdots & \boldsymbol{G}_{M-2} \\ \vdots & \vdots & \ddots & \vdots \\ \boldsymbol{G}_1 & \boldsymbol{G}_2 & \cdots & \boldsymbol{G}_0 \end{bmatrix}, \end{aligned} \tag{17}$$

where $\boldsymbol{G}_i$ is an $\bar{N}\times\bar{N}$ matrix. The discrete Fourier transform (DFT) of $\boldsymbol{G}$ can be computed by [36]

$$\mathcal{F}(\boldsymbol{G}) = \mathcal{C}\left(\bar{\boldsymbol{G}}_0, \bar{\boldsymbol{G}}_1, \cdots, \bar{\boldsymbol{G}}_{M-1}\right), \tag{18}$$

where

$$\begin{aligned}\bar{\boldsymbol{G}}_s &= \sum_{r=0}^{M-1} \boldsymbol{G}_r \exp\left(-\frac{j2\pi rs}{M}\right) \\ &= \sum_{u=0}^{\bar{M}-1} \boldsymbol{G}_{u\left(\frac{M}{\bar{M}}\right)} \exp\left(-\frac{j2\pi us}{\bar{M}}\right). \end{aligned} \tag{19}$$

Let $\beta = \frac{N}{\bar{N}} = \frac{M}{\bar{M}}$, $s = v + \bar{u}\bar{M}$, $v = 0, 1, \cdots, \bar{M}-1$, and $\bar{u} = 0, 1, \cdots, \beta - 1$, then (19) can be simplified as

$$\begin{aligned}\bar{\boldsymbol{G}}_{v+\bar{u}\bar{M}} &= \sum_{u=0}^{\bar{M}-1} \boldsymbol{G}_{u\beta} \exp\left(-\frac{j2\pi u\left(v+\bar{u}\bar{M}\right)}{\bar{M}}\right) \\ &= \sum_{u=0}^{\bar{M}-1} \boldsymbol{G}_{u\beta} \exp\left(-\frac{j2\pi uv}{\bar{M}}\right). \end{aligned} \tag{20}$$

Obviously, (20) can utilize $\bar{M}$-point FFT to compute $\bar{\boldsymbol{G}}_{v+\bar{u}\bar{M}}$. According to (9) and (10), one can easily conclude that $\boldsymbol{G}_{u\beta}$ is a diagonal matrix composed of nonzero elements in its principal diagonal. By utilizing the results of the block circulant matrices theorem [40], if and only if the $\bar{\boldsymbol{G}}_s$ is invertible, the inverse matrix of $\boldsymbol{G}$ can be solved by

$$\begin{aligned}\boldsymbol{G}^{-1} &= \mathcal{C}\left(\boldsymbol{B}_0, \boldsymbol{B}_1, \cdots, \boldsymbol{B}_{M-1}\right) \\ &= \begin{bmatrix} \boldsymbol{B}_0 & \boldsymbol{B}_1 & \cdots & \boldsymbol{B}_{M-1} \\ \boldsymbol{B}_{M-1} & \boldsymbol{B}_0 & \cdots & \boldsymbol{B}_{M-2} \\ \vdots & \vdots & \ddots & \vdots \\ \boldsymbol{B}_1 & \boldsymbol{B}_2 & \cdots & \boldsymbol{B}_0 \end{bmatrix}, \end{aligned} \tag{21}$$

where

$$\boldsymbol{B}_r = \frac{1}{M}\sum_{s=0}^{M-1} \bar{\boldsymbol{G}}_s^{-1} \exp\left(\frac{j2\pi rs}{M}\right), \quad 0 \le r \le M-1, \tag{22}$$

which has a similar structure to (19) and can be simplified by utilizing FFT. Substituting (21) into (8) leads to

$$\begin{bmatrix} \boldsymbol{\gamma}^{(p)}_0 \\ \boldsymbol{\gamma}^{(p)}_1 \\ \vdots \\ \boldsymbol{\gamma}^{(p)}_{M-1} \end{bmatrix} = \begin{bmatrix} \boldsymbol{B}_0 & \boldsymbol{B}_1 & \cdots & \boldsymbol{B}_{M-1} \\ \boldsymbol{B}_{M-1} & \boldsymbol{B}_0 & \cdots & \boldsymbol{B}_{M-2} \\ \vdots & \vdots & \ddots & \vdots \\ \boldsymbol{B}_1 & \boldsymbol{B}_2 & \cdots & \boldsymbol{B}_0 \end{bmatrix} \begin{bmatrix} \boldsymbol{g}^{(p)}_0 \\ \boldsymbol{g}^{(p)}_1 \\ \vdots \\ \boldsymbol{g}^{(p)}_{M-1} \end{bmatrix}, \tag{23}$$

and then (23) can be rewritten in following form

$$\begin{aligned} \boldsymbol{\gamma}^{(p)}_0 &= \boldsymbol{B}_0\boldsymbol{g}^{(p)}_0 + \boldsymbol{B}_1\boldsymbol{g}^{(p)}_1 + \cdots + \boldsymbol{B}_{M-1}\boldsymbol{g}^{(p)}_{M-1} \\ \boldsymbol{\gamma}^{(p)}_1 &= \boldsymbol{B}_{M-1}\boldsymbol{g}^{(p)}_0 + \boldsymbol{B}_0\boldsymbol{g}^{(p)}_1 + \cdots + \boldsymbol{B}_{M-2}\boldsymbol{g}^{(p)}_{M-1} \\ &\vdots \\ \boldsymbol{\gamma}^{(p)}_{M-1} &= \boldsymbol{B}_1\boldsymbol{g}^{(p)}_0 + \boldsymbol{B}_2\boldsymbol{g}^{(p)}_1 + \cdots + \boldsymbol{B}_0\boldsymbol{g}^{(p)}_{M-1}. \end{aligned} \tag{24}$$

Let $\boldsymbol{g}^{(p)}_t$ denotes block time signal, which can be putted into a block delay line in arrays range $t = 0$ to $M-1$ as shown in Fig. 1. The dual Gabor windows $\boldsymbol{\gamma}^{(p)}$ at block time $t \in \{0, 1, \cdots, M-1\}$ can be utilized to derive a block time recursive relation between the current state (the current block

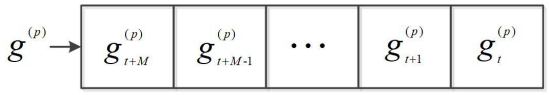

FIGURE 1. Block delay line ($p = 0, 1, \cdots, P-1$).

time signal taking in) and the previous state (the previous block time signal taking out) from the line, so

$$\begin{aligned}
\boldsymbol{\gamma}_0^{(p)}(t) &= \boldsymbol{B}_0\boldsymbol{g}_t^{(p)} + \boldsymbol{B}_1\boldsymbol{g}_{t+1}^{(p)} + \cdots + \boldsymbol{B}_{M-1}\boldsymbol{g}_{t+M-1}^{(p)} \\
\boldsymbol{\gamma}_1^{(p)}(t) &= \boldsymbol{B}_{M-1}\boldsymbol{g}_t^{(p)} + \boldsymbol{B}_0\boldsymbol{g}_{t+1}^{(p)} + \cdots + \boldsymbol{B}_{M-2}\boldsymbol{g}_{t+M-1}^{(p)} \\
&\vdots \\
\boldsymbol{\gamma}_{M-1}^{(p)}(t) &= \boldsymbol{B}_1\boldsymbol{g}_t^{(p)} + \boldsymbol{B}_2\boldsymbol{g}_{t+1}^{(p)} + \cdots + \boldsymbol{B}_0\boldsymbol{g}_{t+M-1}^{(p)},
\end{aligned} \tag{25}$$

then, at block time $t+1$, the dual Gabor windows $\boldsymbol{\gamma}^{(p)}$ can be expressed as follows

$$\begin{aligned}
\boldsymbol{\gamma}_0^{(p)}(t+1) &= \boldsymbol{B}_0\boldsymbol{g}_{t+1}^{(p)} + \boldsymbol{B}_1\boldsymbol{g}_{t+2}^{(p)} + \cdots + \boldsymbol{B}_{M-1}\boldsymbol{g}_{t+M}^{(p)} \\
\boldsymbol{\gamma}_1^{(p)}(t+1) &= \boldsymbol{B}_{M-1}\boldsymbol{g}_{t+1}^{(p)} + \boldsymbol{B}_0\boldsymbol{g}_{t+2}^{(p)} + \cdots + \boldsymbol{B}_{M-2}\boldsymbol{g}_{t+M}^{(p)} \\
&\vdots \\
\boldsymbol{\gamma}_{M-1}^{(p)}(t+1) &= \boldsymbol{B}_1\boldsymbol{g}_{t+1}^{(p)} + \boldsymbol{B}_2\boldsymbol{g}_{t+2}^{(p)} + \cdots + \boldsymbol{B}_0\boldsymbol{g}_{t+M}^{(p)}.
\end{aligned} \tag{26}$$

Hence, the following relationship of the dual Gabor windows $\boldsymbol{\gamma}^{(p)}$ at block time t and block time $t+1$ can be obtained as

$$\begin{aligned}
\boldsymbol{\gamma}_0^{(p)}(t+1) &= \boldsymbol{\gamma}_1^{(p)}(t) + \boldsymbol{B}_{M-1}\left(\boldsymbol{g}_{t+M}^{(p)} - \boldsymbol{g}_t^{(p)}\right) \\
\boldsymbol{\gamma}_1^{(p)}(t+1) &= \boldsymbol{\gamma}_2^{(p)}(t) + \boldsymbol{B}_{M-2}\left(\boldsymbol{g}_{t+M}^{(p)} - \boldsymbol{g}_t^{(p)}\right) \\
&\vdots \\
\boldsymbol{\gamma}_{M-2}^{(p)}(t+1) &= \boldsymbol{\gamma}_{M-1}^{(p)}(t) + \boldsymbol{B}_1\left(\boldsymbol{g}_{t+M}^{(p)} - \boldsymbol{g}_t^{(p)}\right) \\
\boldsymbol{\gamma}_{M-1}^{(p)}(t+1) &= \boldsymbol{\gamma}_0^{(p)}(t) + \boldsymbol{B}_0\left(\boldsymbol{g}_{t+M}^{(p)} - \boldsymbol{g}_t^{(p)}\right).
\end{aligned} \tag{27}$$

Steps: (a) reset all the units of the block delay line before the recursion begins at $t = 0$ and set $\boldsymbol{\gamma}_i^{(p)}$ ($p = 0, 1, \cdots, P-1$, $i = 0, 1, \cdots, M-1$) to zero; (b) if $t = M-1$, all of the block units of $\boldsymbol{g}^{(p)}(p=0, 1, \cdots, P-1)$ are inputted into delay line in series and $\boldsymbol{\gamma}^{(p)}$ can be computed by (27); (c) when $t = M$, due to the periodicity of $\boldsymbol{g}^{(p)}$, the recursive process goes into a stable state in (27). The above procedure is listed as Algorithm 1 which can be implemented using the parallel lattice structure as shown in Fig. 2.

IV. COMPUTATIONAL COMPLEXITY ANALYSIS AND COMPARISON

Since the computational time of the proposed parallel algorithm is equal to the computational time of each single unified parallel lattice module, while the computational time of a serial algorithm is equal to the total computational time of each of its modules connected in series.

The computational complexity for computing $\boldsymbol{G}^{-1}$ of the proposed algorithm is of the order of $O\left(2L\log_2(\bar{M})\right)$. In Fig. 2, each unified parallel channel carries $\bar{N}$ additions and

Algorithm 1 Block Time-Recursive Method for Computing Dual Gabor Windows of M-DGT

(a) Let $p = 0 : P-1, i = 0 : \beta-1, j = 0 : M-1, t = 0$.
  $\boldsymbol{\gamma}_i^{(p)} = 0$.
(b) ***For*** $p = 0 : P-1, i = 0 : M-1$
  $\boldsymbol{\gamma}_i^{(p)}(t+1) = \boldsymbol{\gamma}_{i+1}^{(p)}(t) + \boldsymbol{B}_{M-i-1}\left(\boldsymbol{g}_{t+M}^{(p)} - \boldsymbol{g}_t^{(p)}\right)$.
  if $(t = \bar{M}-1)$
    break.
  else
    $t = t+1$.
    $\boldsymbol{g}_{t+M}^{(p)} = \boldsymbol{g}_t^{(p)}$.
  endif
Endfor

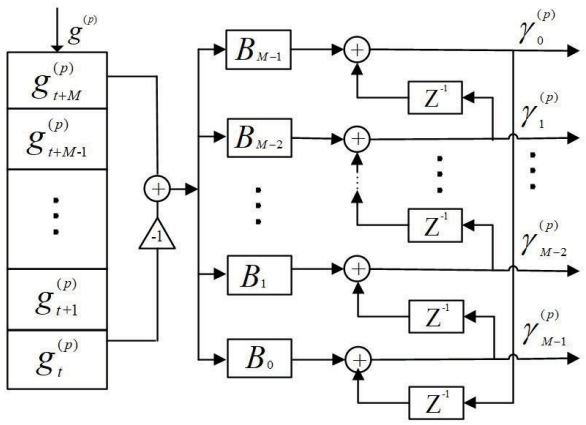

FIGURE 2. Parallel lattice structure of block time-recursive method for computing dual Gabor windows of M-DGT ($p = 0, 1, \cdots, P-1$).

$\bar{N}$ multiplications at each block time. Therefore, the computational complexity of the proposed algorithm is of the order of

$$O\left(L + 2L\log_2(\bar{M})\right). \tag{28}$$

A comparison of the computational complexity of the proposed algorithm and other algorithms [31]–[33] is given in Table 1.

V. COMPUTATIONAL EXAMPLES AND RESULTS

Example 1: In this example, we compare the proposed algorithm with other algorithms in terms of numerical complexity. According to Table 1, Table 2 gives a numerical comparison of the computational complexity in terms of the total number of multiplications between the proposed algorithm and the other three algorithms using different sets of Gabor sampling patterns. It can be seen from Table 2 that the computational complexity of the proposed algorithm is far less than those of the other three serial algorithms.

Example 2: In this example, the proposed method was used to compute the dual (analysis) windows. Four Gaussian windows $g^{(p)}(k)$ are defined in (29) and plotted in Fig. 3, where $L = 256$, $P = 4$, and $\boldsymbol{\sigma} = [\sigma_0, \sigma_1, \sigma_2, \sigma_3] = [2, 16, 32, 64]$.

$$g^{(p)}(k) = 2^{-p/2} \cdot \exp\left(-\frac{[k - 0.5(L-1)]^2}{\sigma_p^2}\right), \tag{29}$$

TABLE 1. Comparison of computational complexity between proposed algorithm and other algorithms.

Algorithms	Computational complexity
[31]	$PMN + PL^3 + 2PL^2$
[32]	$P\left(\bar{M}\bar{N}\right)^3 + 2PL\left(\bar{M}\bar{N}\right)^2 + PL\left(\bar{M}\bar{N}\right)$
[33]	$2PL\bar{M}^2 + P\bar{N}\bar{M}^3 + PL\bar{M}$
Proposed algorithm	$L + 2L\log_2(\bar{M})$

TABLE 2. Numeric comparison of total number of multiplications between proposed algorithm and other algorithms.

P	L	M	N	β	Total number of multiplications [31]	[32]	[33]	Proposed algorithm
2	128	8	16	1	4260096	12615680	51200	896
		16	32	4	4260864	598016	10240	640
		32	64	16	4263936	35840	2624	384
4	256	16	16	1	67634176	201588736	802816	2304
		32	64	8	67641344	2260992	38912	1280
		64	128	32	67665920	141312	10368	768
8	512	32	16	1	1077940224	3223322624	12713984	5632
		64	128	16	1078001664	8781824	151552	2560
		128	256	64	1078198272	561152	41216	1536

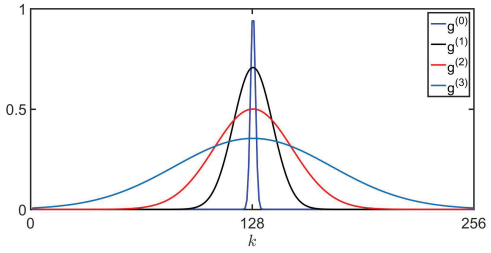

FIGURE 3. Four Gaussian windows $g^{(p)}(k)$ ($p = 0, 1, \cdots, 3$).

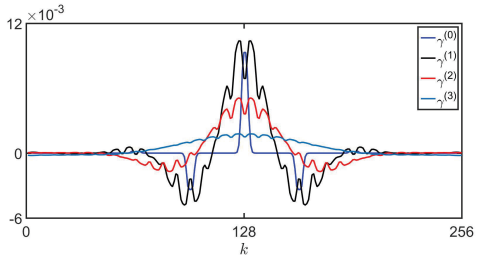

FIGURE 4. Dual Gabor windows $\gamma^{(p)}(k)$ with Gabor sampling rate $\beta = 4$ ($M = 32$, $N = 32$).

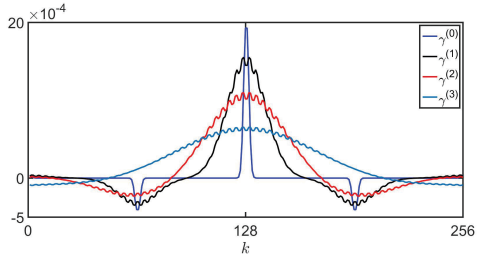

FIGURE 5. Dual Gabor windows $\gamma^{(p)}(k)$ with Gabor sampling rate $\beta = 16$ ($M = 64$, $N = 64$).

where $0 \le p \le P-1$ and $0 \le k \le L-1$. Figs. 4-7 show examples of different dual Gabor windows corresponding to given Gaussian windows $g^{(p)}(k)$ in (29) under different Gabor sampling schemes. Fig. 4 shows the dual Gabor windows $\gamma^{(p)}(k)$ computed using $M = 32$ and $N = 32$, with Gabor sampling rate $\beta = 4$. Figs. 5-7 show the dual Gabor windows $\gamma^{(p)}(k)$ computed with $\beta = 16$ ($M = 64, N = 64$), $\beta = 32$ ($M = 128, N = 128$), and $\beta = 256$ ($M = 256, N = 256$), respectively. From the Figs. 4-7, as the Gabor sampling rate increases, the dual Gabor windows $\gamma^{(p)}(k)$ becomes more similar to its synthesis windows $g^{(p)}(k)$.

Example 3: Fig. 8 shows a segment of electrocardiogram (ECG) signal $x(k)$ (from MIT-BIH Arhythmia Database [41]), with samples length $L = 512$. The signal $x(k)$ is analyzed by the M-DGT with a narrow window and a wide window by setting $P = 2$, $M = 256$, $N = 256$, and $\sigma = [2, 100]$. The Gabor time-frequency spectra shown in Figs. 9-10 are computed by using a narrow window and a wide window, respectively, where the Gabor time-frequency spectrum $S^{(p)}(m, n)$ is defined by (30)

$$S^{(p)}(m,n) = \left|c^{(p)}(m,n)\right|^2, \quad p = 0, 1, \tag{30}$$

where $0 \le m \le M-1$ and $0 \le n \le N-1$. The combined Gabor time-frequency spectrum $S(m, n)$ defined by (31) and shown in Fig. 11 is computed by the geometric average of the narrow Gabor time-frequency spectrum $S^{(0)}(m, n)$ and the wide Gabor time-frequency spectrum $S^{(1)}(m, n)$. Note that the

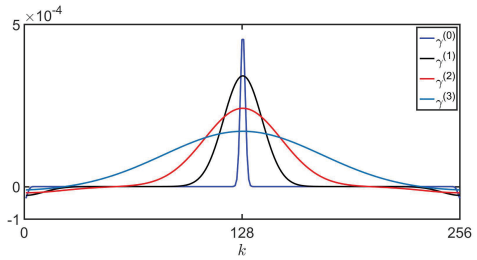

FIGURE 6. Dual Gabor windows $\gamma^{(p)}(k)$ with Gabor sampling rate $\beta = 64$ ($M = 128$, $N = 128$).

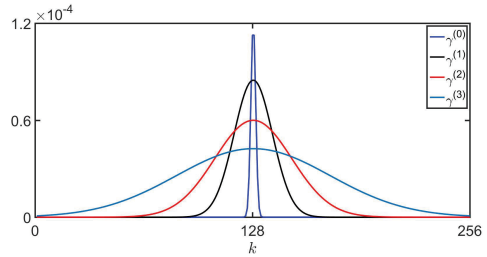

FIGURE 7. Dual Gabor windows $\gamma^{(p)}(k)$ with Gabor sampling rate $\beta = 256$ ($M = 256$, $N = 256$).

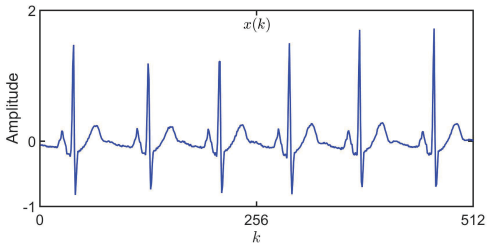

FIGURE 8. A segment of ECG signal.

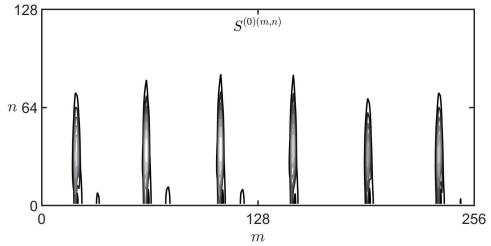

FIGURE 9. Gabor time-frequency spectrum using a narrow window.

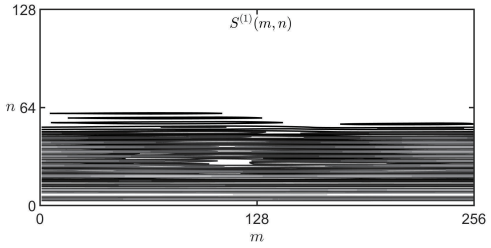

FIGURE 10. Gabor time-frequency spectrum using a wide window.

energy of the signal $x(k)$ is concentrated on specific discrete-time and discrete-frequency

$$S(m, n) = S^{(0)}(m, n) \times S^{(1)}(m, n) \tag{31}$$

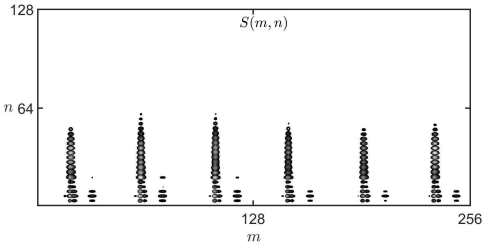

FIGURE 11. Gabor time-frequency spectrum using a narrow window and a wide window.

points. The original signal $x(k)$ is also reconstructed by the proposed algorithm as plotted in Fig. 11, the reconstruction error is less than 10^{-17} which is close to virtually error-free reconstruction.

VI. CONCLUSION

In multiwindow Gabor analysis, solving the dual Gabor windows for a given multiwindow Gabor frame is an important issue in the M-DGT. Traditional methods to compute dual Gabor windows based on minimum ℓ_2 norm, require the inverse matrix computation of a frame operator with a high computational complexity especially if the matrix dimensions are high which could also lead to numerical instability. To address this issue, an efficient algorithm for computing dual Gabor windows in the M-DGT based on the canonical dual Gabor frame has been presented, which can avoid computing the inverse matrix of the frame operator. According to the properties of the block circulant matrix, the inverting frame matrix can be solved by utilizing the FFT and the parallel lattice structure of the block time-recursive method can be used to design and implement the proposed algorithm. Computational complexity analysis and comparison have clearly indicated that the proposed algorithm can provide a fast approach to compute the dual Gabor windows as compared to the other three existing methods.

REFERENCES

[1] D. Gabor, "Theory of communication," *J. Inst. Elect. Eng. III, Radio Commun. Eng.*, vol. 93, no. 3, pp. 429–457, Nov. 1946.
[2] L. Tao and H. K. Kwan, "Parallel lattice structures of block time-recursive discrete Gabor transform and its inverse transform," *Signal Process.*, vol. 88, no. 2, pp. 407–414, Feb. 2008.
[3] C. Lin, L. Tao, and H. K. Kwan, "Parallel-computing-based implementation of fast algorithms for discrete Gabor transform," *IET Signal Process.*, vol. 9, no. 7, pp. 546–552, Sep. 2015.
[4] L. Tao and H. K. Kwan, "Novel DCT-based real-valued discrete Gabor transform and its fast algorithms," *IEEE Trans. Signal Process.*, vol. 57, no. 6, pp. 2151–2164, Jun. 2009.
[5] L. Tao and H. K. Kwan, "Multirate-based fast parallel algorithms for DCT-kernel-based real-valued discrete Gabor transform," *Signal Process.*, vol. 92, no. 3, pp. 679–684, Mar. 2012.
[6] L. Tao and H. K. Kwan, "Block time-recursive real-valued discrete Gabor transform implemented by unified parallel lattice structure," *IEICE Trans. Inf. Syst.*, vol. E88-D, no. 7, pp. 1472–1478, Jul. 2005.
[7] L. Tao and H. K. Kwan, "Fast parallel approach for 2-D DHT-based real-valued discrete Gabor transform," *IEEE Trans. Image Process.*, vol. 18, no. 12, pp. 2790–2796, Dec. 2009.
[8] L. Tao and H. K. Kwan, "Multirate-based fast parallel algorithms for 2-D DHT-based real-valued discrete Gabor transform," *IEEE Trans. Image Process.*, vol. 21, no. 7, pp. 3306–3311, Jul. 2012.

[9] N. Delprat, "Global frequency modulation laws extraction from the Gabor transform of a signal: A first study of the interacting components case," *IEEE Trans. Speech Audio Process.*, vol. 5, no. 1, pp. 64–71, Jan. 1997.
[10] S. Agili, D. B. Bjornberg, and A. Morales, "Optimized search over the Gabor dictionary for note decomposition and recognition," *J. Franklin Inst.*, vol. 344, no. 7, pp. 969–990, Sep. 2007.
[11] B. Ricaud, G. Stempfel, B. Torrésani, C. Wiesmeyr, H. Lachambre, and D. Onchis, "An optimally concentrated Gabor transform for localized time-frequency components," *Adv. Comput. Math.*, vol. 40, no. 3, pp. 683–702, Jun. 2014.
[12] E. Erçelebi, "Speech enhancement based on the discrete Gabor transform and multi-notch adaptive digital filters," *Appl. Acoust.*, vol. 65, no. 8, pp. 739–762, Aug. 2004.
[13] Y. Zhang and H. Zhang, "Doppler ultrasound spectral enhancement using the Gabor transform-based spectral subtraction," *IEEE Trans. Ultrason., Ferroelectr., Freq. Control*, vol. 52, no. 10, pp. 1861–1868, Oct. 2005.
[14] L. Tao and H. K. Kwan, "Noise reduction for NMR FID signals via oversampled real-valued discrete Gabor transform," *IEICE Trans. Inf. Syst.*, vols. E88–D, no. 7, pp. 1511–1518, Jul. 2005.
[15] B. S. Manjunath and W. Y. Ma, "Texture features for browsing and retrieval of image data," *IEEE Trans. Pattern Anal. Mach. Intell.*, vol. 18, no. 8, pp. 837–842, Aug. 1996.
[16] J. Chen, T. N. Pappas, A. Mojsilovic, and B. E. Rogowitz, "Adaptive perceptual color-texture image segmentation," *IEEE Trans. Image Process.*, vol. 14, no. 10, pp. 1524–1536, Oct. 2005.
[17] Y. Shi, X. Yang, and Y. Guo, "Translation invariant directional framelet transform combined with Gabor filters for image denoising," *IEEE Trans. Image Process.*, vol. 23, no. 1, pp. 44–55, Oct. 2013.
[18] Z.-S. Zhao, L. Zhang, M. Zhao, Z.-G. Hou, and C.-S. Zhang, "Gabor face recognition by multi-channel classifier fusion of supervised kernel manifold learning," *Neurocomputing*, vol. 97, pp. 398–404, Nov. 2012.
[19] L. Dora, S. Agrawal, R. Panda, and A. Abraham, "An evolutionary single Gabor kernel based filter approach to face recognition," *Eng. Appl. Artif. Intell.*, vol. 62, pp. 286–301, Jun. 2017.
[20] J. Zou, C. C. Liu, Y. Zhang, and G. F. Lu, "Object recognition using Gabor co-occurrence similarity," *Pattern Recognit.*, vol. 46, no. 1, pp. 434–448, Jan. 2013.
[21] O. Oktay, G. E. Pfander, and P. Zheltov, "Reconstruction of the scattering function of overspread radar targets," *IET Signal Process.*, vol. 8, no. 9, pp. 1018–1024, Dec. 2014.
[22] S. Qian and D. Chen, "Discrete Gabor transform," *IEEE Trans. Signal Process.*, vol. 41, no. 7, pp. 2429–2438, Jul. 1993.
[23] S. Qian and D. Chen, "Optimal biorthogonal analysis window function for discrete Gabor transform," *IEEE Trans. Signal Process.*, vol. 42, no. 3, pp. 694–697, Mar. 1994.
[24] H. Bölcskei, "A necessary and sufficient condition for dual Weyl-Heisenberg frames to be compactly supported," *J. Fourier Anal. Appl.*, vol. 5, no. 5, pp. 409–419, Sep. 1999.
[25] O. Christensen, O. K. Hong, and R. Y. Kim, "Gabor windows supported on $[-1, 1]$ and dual windows with small support," *Adv. Comput. Math.*, vol. 28, no. 4, pp. 525–545, May 2012.
[26] P. L. Søndergaard, "Efficient algorithms for the discrete Gabor transform with a long FIR window," *J. Fourier Anal. Appl.*, vol. 18, no. 3, pp. 456–470, Jun. 2012.
[27] R. Li and L. Tao, "Fast algorithm for computing analysis windows in real-valued discrete Gabor transform," *IEICE Trans. Inf. Syst.*, vol. E99-D, no. 6, pp. 1682–1685, Jun. 2016.
[28] J. Wexler and S. Raz, "Discrete Gabor expansions," *Signal Process.*, vol. 21, no. 3, pp. 207–220, Nov. 1990.
[29] T. Strohmer, "Numerical algorithms for discrete Gabor expansions," in *Gabor Analysis and Algorithms*, H. G. Feichtinger and T. Strohmer, Eds. Boston, MA, USA: Birkhäuser, 1998, ch. 8, pp. 267–294.
[30] I. Daubechies, H. J. Landau, and Z. Landau, "Gabor time-frequency lattices and the Wexler-Raz identity," *J. Fourier Anal. Appl.*, vol. 1, no. 4, pp. 437–478, Nov. 1994.
[31] S. Li, "Discrete multi-Gabor expansions," *IEEE Trans. Inf. Theory*, vol. 45, no. 6, pp. 1954–1967, Sep. 1999.
[32] L. Tao, G. H. Hu, and H. K. Kwan, "Multiwindow real-valued discrete Gabor transform and its fast algorithms," *IEEE Trans. Signal Process.*, vol. 63, no. 20, pp. 5513–5524, Oct. 2015.
[33] R. Li and J.-B. Liu, "Fast approach for analysis windows computation of multiwindow discrete Gabor transform," *IEEE Access*, vol. 6, pp. 45681–45689, Aug. 2018.
[34] R. Li, L. Tao, and H. K. Kwan, "Efficient discrete Gabor transform with weighted linear combination of analysis windows," *Electron. Lett.*, vol. 52, no. 9, pp. 772–774, Feb. 2016.
[35] A. Akan and L. F. Chaparro, "Multi-window Gabor expansion for evolutionary spectral analysis," *Signal Process.*, vol. 63, no. 3, pp. 249–262, Dec. 1997.
[36] T. Werther, Y. C. Eldar, and N. K. Subbanna, "Dual Gabor frames: Theory and computational aspects," *IEEE Trans. Signal Process.*, vol. 53, no. 11, pp. 4147–4158, Nov. 2005.
[37] J. Zhou, H.-B. Wang, L. Tao, and L. Zhao, "Dual window computation based on discrete Fourier transform and parallel lattice structures of block time–recursive in discrete Gabor transform," *Acta Electron. Sinica*, vol. 40, no. 9, pp. 1839–1843, Sep. 2012.
[38] R. Li and J. Zhou, "Sparse Gabor time-frequency representation based on $\ell_{1/2}$-ℓ_2 regularization," *Circuits, Syst., Signal Process.*, vol. 38, no. 10, pp. 4700–4722, Oct. 2019.
[39] S. Qiu and H. G. Feichtinger, "Discrete Gabor structures and optimal representations," *IEEE Trans. Signal Process.*, vol. 43, no. 10, pp. 2258–2268, Oct. 1995.
[40] R. Vescovo, "Inversion of block-circulant matrices and circular array approach," *IEEE Trans. Antennas Propag.*, vol. 45, no. 10, pp. 1565–1567, Oct. 1997.
[41] T. Penzel, G. B. Moody, R. G. Mark, A. L. Goldberger, and J. H. Peter, "The apnea-ECG database," in *Proc. Comput. Cardiol.*, Cambridge, MA, USA, Sep. 2000, pp. 255–258.

RUI LI received the B.S. degree in computer science and technology from the Anhui University of Science and Technology, in 2009, the M.S. degree in computer science from Anhui University, China, in 2012, and the Ph.D. degree in applied computer technology from Anhui University, China, in 2016. He is currently a Lecturer with the College of Information and Network Engineering, Anhui Science and Technology University, China. His main research interests include time-frequency analysis, image processing, and pattern recognition.

HON KEUNG KWAN (M'81–SM'86–LSM'18) received the D.I.C. and Ph.D. degree in electrical engineering (signal processing) from Imperial College London, U.K., in 1981. His previous experiences include working as a Design Engineer in Electronics and Computer Memory Industry, from 1977 to 1978; and has been a Faculty Member with the Department of Electronic Engineering, The Hong Kong Polytechnic University, since 1981, and then with the Department of Electrical and Electronic Engineering, The University of Hong Kong. He subsequently joined the University of Windsor and holds the rank of Professor in electrical and computer engineering, since 1989. His current research interests include on digital filter and deep neural network design. Dr. Kwan is a licensed Professional Engineer (Ontario), a Chartered Electrical Engineer, U.K., and was elected in 1996 a Fellow of the Institution of Engineering and Technology, U.K. He had served as the Chair and various officers in each of the Digital Signal Processing Technical Committee and the Neural Systems and Applications Technical Committee of the IEEE Circuits and Systems Society.